THE JOURNAL OF PROSTHETIC DENTISTRY

RESEARCH AND EDUCATION

# Osteogenesis ability of CAD-CAM biodegradable polylactic acid scaffolds for reconstruction of jaw defects

Mohamed H. Helal, BDS, MS,[a] Hebatullah D. Hendawy,[b] Rowan A. Gaber,[c] Nourhan R. Helal,[d] and Moustafa N. Aboushelib, DDS, MS, PhD[e]

## ABSTRACT

**Statement of problem.** Reconstruction of alveolar bony defects is difficult using grafting materials in a powder form. A biodegradable scaffold material might simplify the procedure.

**Purpose.** The purpose of this in vivo study was to evaluate osteogenesis ability of a biodegradable CAD-CAM–fabricated polylactic acid (PLA) scaffold enriched with calcium phosphate salts including hydroxyapatite (HA) and beta tricalcium phosphate (β-TCP) used to reconstruct mandibular defects in a dog model.

**Material and methods.** Surgical defects were made bilaterally in the mandible of male beagle dogs. Computerized tomography images were obtained for determination of the 3-dimensional shape of the defects after 3 months of healing. Porous PLA scaffolds were fabricated by milling custom-made CAD-CAM blocks into the desired shape. After milling, half of the scaffolds were prepared by filling the pores of the scaffolds by a mixture of HA and β-TCP. Scaffolds were inserted in the mandibular defects bilaterally. After a healing time of 8 weeks, the bone-scaffold interface was analyzed histomorphometrically to detect the amount of new bone formation. Stained histological sections were examined using a computer software and depth of new bone formation was assessed (n=14, α=.05).

**Results.** Histomorphometric analysis revealed that enriched scaffolds with calcium phosphates had significantly (t=4.4, $P<.001$) higher amounts of new bone formation (1.3 ±0.33 mm) compared with the controls (0.7 ±0.39 mm). Average new bone growth in enriched scaffolds was 1.3 mm while almost half this value was observed in uncoated scaffolds, 0.7 mm.

**Conclusions.** Within the limitations of this animal study, HA and β-TCP enhanced osteogenesis ability of CAD-CAM–fabricated PLA scaffolds. (J Prosthet Dent 2019;121:118-23)

Alveolar ridge resorption due to prolonged edentulism and bone atrophy results from failure of bone augmentation after tooth extraction, especially in the buccal regions, leading to loss in alveolar volume, vertically and horizontally. Absence of sufficient amount of bone tissue needed for the support of oral implants may complicate the rehabilitation plan and influence the treatment modality. Therefore, bone augmentation at the recipient site must be performed before oral rehabilitation to provide dental implants with sufficient stability.[1-5]

Many bone graft materials are currently available, including autogenous grafts which are generally assumed to be the gold standard[6,7] because of an absence of immune response.[5] However, there are disadvantages such as inflammation, insufficiency of bone quantity in the donor site,[7,8] and risk of vascular and neurological injuries. Other materials used include allograft, xenograft, and synthetic biomaterial composites.[5-8]

Three-dimensional (3D) scaffolds have the advantage of maintaining shape during the healing time better than direct grafting materials that are delivered in powder form and suffer from shape collapse due to soft tissue pressure and functional stresses. Depending on chemistry, molecular weight, solubility, shape, and other mechanical properties, various scaffold materials exhibit different biological responses.[9] Synthetic scaffolds as polymers, ceramics, metals, and composites have

[a]Resident, Oral Medicine, Diagnosis, Radiology, and Periodontology, Faculty of Dentistry, Tanta University, Alexandria, Egypt.
[b]Predoctoral student, Biomaterials Laboratory, Faculty of Dentistry, Alexandria University, Alexandria, Egypt.
[c]Predoctoral student, Biomaterials Laboratory, Faculty of Dentistry, Alexandria University, Alexandria, Egypt.
[d]Predoctoral student, Biomaterials Laboratory, Faculty of Dentistry, Alexandria University, Alexandria, Egypt.
[e]Professor, Biomaterials, Faculty of Dentistry, Alexandria University, Alexandria, Egypt.

## Clinical Implications

CAD-CAM biodegradable scaffolds could enhance reconstruction of alveolar bony defects offering an easier surgical approach and more predictable results.

superior mechanical properties and straightforward processing techniques, making them a favorable choice for ridge augmentation.[10] Despite of the brittleness, low fracture strength, and less predictable degradation rates, calcium phosphate ceramics are the most commonly used grafting substitutes because of their biocompatibility, biodegradability, osteoconductivity, and osteoinductivity.[11-13] The biocompatibility of calcium phosphate ceramics can be related to its similarity to the biominerals that are naturally found as part of bone or teeth.[13,14] Also, having the ability to form a bioactive apatite layer on their surfaces enhances their osseointegration capacity.[11,13] Synthetic hydroxyapatite (HA) and beta tricalcium phosphate (β-TCP) are the most common clinically used synthetic ceramics.[13-16]

Polylactic acid (PLA), an aliphatic polyester derived from lactic acid (2-hydroxypropionic acid), has important medical applications. Besides its biodegradability, PLA is an inexpensive and easily fabricated material which makes it more preferable than other traditional biodegradable medical polymers.[17,18] When PLA is hydrolyzed, lactic acid is produced which is metabolized naturally making it nontoxic and biocompatible.[18,19] Moreover, PLA and its copolymers, such as PLA polyethylene glycol block copolymer and PLA-p-dioxanone-polyethylene glycol block copolymer, show the ability to carry bone morphogenetic proteins to induce new bone formation.[17] In one experiment, low-molecular-weight PLA was mixed with bone morphogenetic proteins to form a composite and then placed in bony defects. The results showed successful new bone formation during degradation of the PLA. However, the quantity of bone formed was small.[17-20] PLA copolymers were used to increase bone formation.[21]

Traditionally, surgeons have estimated the required amount and shape of a bone graft from radiographs, decided the final shape, and manually cut the scaffold into the desired shape during the operation.[22] However, this approach is complicated and time-consuming, and the size and shape of bone graft can be highly inaccurate as it depends heavily on the surgeon's skill to shape delicate 3D shapes manually.[23] Computer-aided design and computer-aided manufacturing (CAD-CAM) offer new solutions for planning bone reconstructive surgery with considerations to the esthetic, prosthetic, and functional demands.[24,25]

Fabrication of 3D custom-made scaffolds is now possible using a variety of materials and techniques. In combination with accurate imaging techniques, the design and construction of CAD-CAM scaffolds has become a straightforward procedure.[22,23] Few studies have evaluated custom-made scaffolds for alveolar ridge augmentation.[24-26] One study successfully showed that porous CAD-CAM custom-made zirconia scaffolds enriched with nano-HA fillers resulted in higher volume bone formation.[27] However, for some clinical applications, it may be desirable to use biodegradable scaffolds.

The purpose of this in vivo study was to evaluate the osteogenesis ability of biodegradable CAD-CAM scaffolds fabricated from PLA and enriched with calcium phosphate particles (HA and β-TCP). The null hypothesis was that calcium phosphate–enriched scaffold would not enhance osteogenesis ability in a dog model.

## MATERIAL AND METHODS

PLA particles were mixed with 75 wt% sodium chloride particles of 2 average sizes (50 μm and 500 μm), and 10% polyethylene glycol was added as a binder. After injection molding at 190°C in the desired block size (150×30 mm), the blocks were stored under water to dissolve the salt particles, leaving the required porosity behind. The 28 scaffolds were numbered from 1 to 28, and systematic random sampling was used with assistance of a random number generator (Microsoft Mathematics; Microsoft Corp) to divide the scaffolds into 2 equal groups. Half of the scaffolds were enriched with a calcium phosphate mixture by immersing into a 25 wt% suspension of mixture of 50% nano-hydroxyapatite and 50% β-TCP in a solution of 70% ethyl alcohol as a carrier. Drying of the scaffolds was achieved by heating each scaffold under a temperature of 60°C for 180 minutes. This process was repeated 3 times to ensure proper filling of the pores. Evaluation of average pore size and distribution was achieved by mercury porosimetry. Elemental surface composition was determined by radiograph diffraction analysis. The density of the prepared PLA scaffolds enriched with (HA and β-TCP) was compared with the theoretical density of fully dense PLA (1.2 to 1.4 g/cm$^3$).

This study was approved by the research and ethics Committee of Tanta University stating conditions and restrictions to conduct and publish studies, including animal models according to research guidelines. Twenty-eight adult male 2-year-old beagle dogs weighing approximately 10 to 12 kg were examined by the animal-house veterinarian to exclude disease and maintain balanced diet consisting of milk, broth, and meat throughout the study period. The animals were housed in individual stainless steel cages in an animal room. Proper ventilation and a 12-hour light/dark cycle were applied. The animals were given free access to water throughout the study. The animals were routinely observed, acclimatized, and divided into 2 groups before surgery by the same systematic random sampling technique.

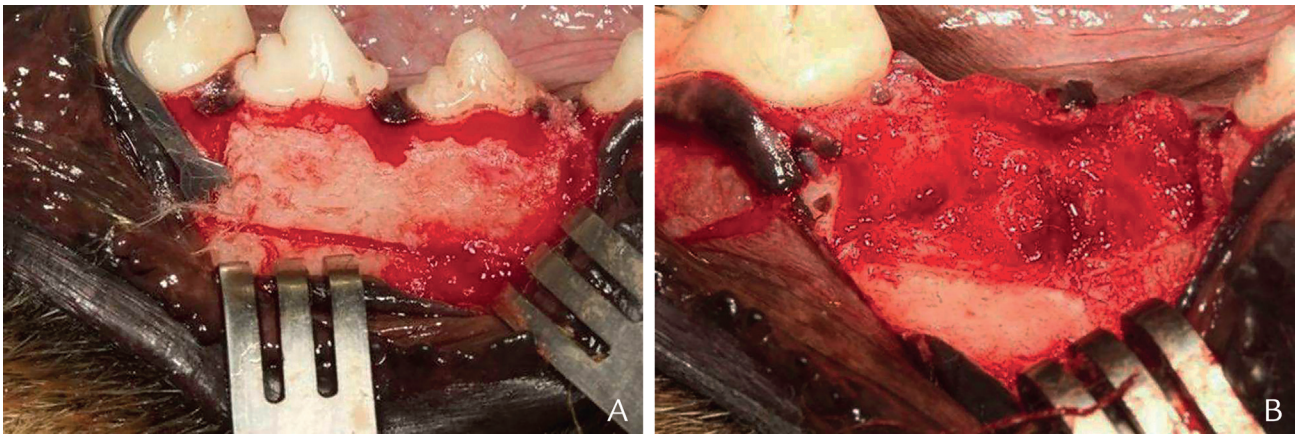


**Figure 1.** A, Exposure of jaw and marking defect size by piezosurgery. B, Final defect size before wound closure.

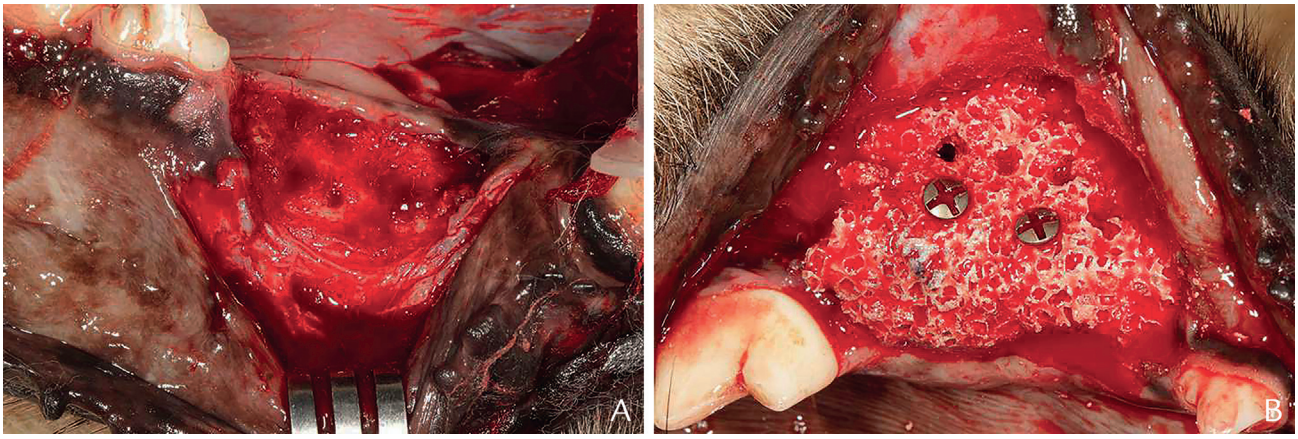


**Figure 2.** A, Defect size exposed after 3 months of healing showing rounding of defect edges. B, Insertion and fixation of scaffolds using titanium screws. Notice match with defect margins.

Each animal received a dose of antibiotics (ampicillin 25 mg/kg body weight) immediately before the operation to avoid postoperative infection. All surgeries were performed under sterile conditions in a veterinary operating theater by an experienced surgeon (M.H.H.). The dogs were preanesthetized with subcutaneous injection of atropine (0.05 mg/kg; Kwang Myung Pharmaceutical). Induction of anesthesia was performed after 10 minutes of premedication by intravenous administration of a mixed xylazine of 2 mg/kg (Xyla-Ject; Adwia Pharmaceuticals) and ketamine hydrochloride of 5.5 mg/kg (KETAMAX-50; Troikaa Pharma) administered in the cephalic vein of the forelimb and maintained by inhalation anesthesia.

Soft tissue flaps were reflected to expose the premolar-molar region of the mandible with a minimum amount of trauma. The entire alveolar segment including buccal and lingual plates of bone were cut using a piezosurgery device (Piezotome Solo LED; Acteon), and involved teeth were removed leaving a 2×1×1-cm 3D defect size. Prophylactic antibiotics were administered intramuscularly (20 mg/kg of cefazolin sodium; Yuhan), and the surgical site was sprayed with topical 0.2% chlorhexidine solution (Fig. 1).

After 3 months of healing time, Digital Imaging and Communications in Medicine (DICOM) files obtained from cone beam computer tomography were transferred to an open-access CAD-CAM software (CAMWorks; Geometric Americas), and the design of the required PLA scaffold was reconstructed to accurately fit the modeled bony defect. The scaffold was designed to restore normal contour of the resected ridge. A 5-axis dry milling unit (DWX-51D 5; Roland) was used to mill the prepared blocks into the required. The scaffolds were sterilized using gamma rays. The animals were prepared as previously described, and the scaffolds were fixed in the healed jaw defect using titanium fixation screws (2 mm in diameter and 16 mm in length; Jeil Medical Corp), and the surgical flap was repositioned and sutured (Fig. 2).

After 8 weeks, the animals were sacrificed with an overdose of thiopental sodium, and mandibular blocks were dissected from the animals. The blocks were immediately fixed in 4% buffered formaldehyde for 1 week.

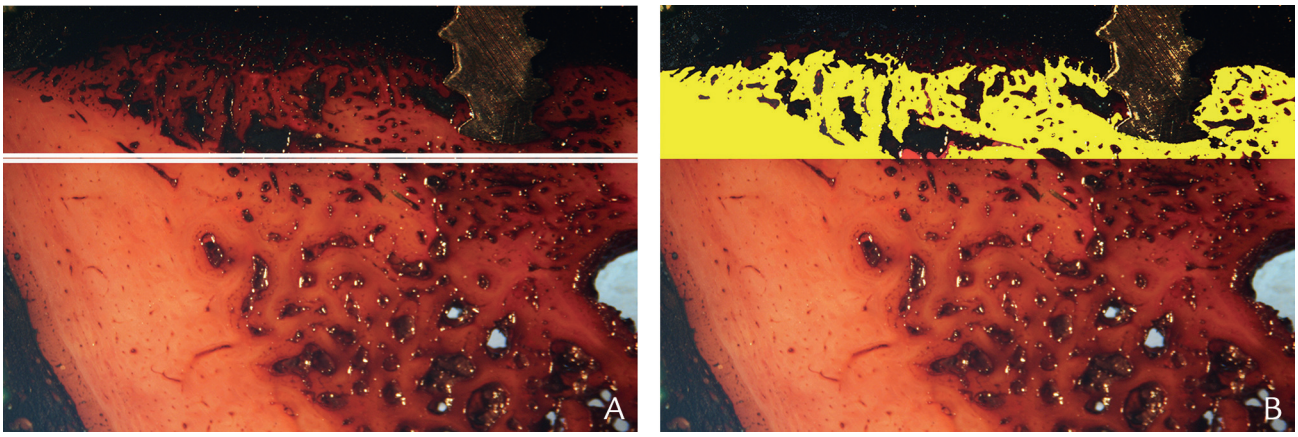


**Figure 3.** A, Stained histological section demarcating area between scaffold and surrounding bone defect (white area). Notice position of fixation screw. B, Area of mineralized new bone isolated and stained yellow to allow precise measuring of depth of new bone formation measured from surface of defect wall.

**Table 1.** New bone formation, porosity, pore size range, and density of tested groups

| Test Group | New Bone Formation (mm) (Mean ±SD) | Porosity (%) | Pore Size Ranges (μm) | Density (g/cm$^3$) |
|---|---|---|---|---|
| Control | 1.7 ±0.57 | 77 | 59-540 | 0.35 |
| HA enriched | 4.2 ±0.71 | 43 | 28-211 | 0.68[3] |

HA, hydroxyapatite; SD, standard deviation.

Then, the specimens were dehydrated in ascending ethanol concentrations (50%, 70%, 90%, and 100%) using a dehydration system (ASP 300S; Leica Biosystems) under agitation and vacuum. The blocks were embedded in transparent chemically polymerized methyl methacrylate resin and cut along the long axis of the blocks in a coronal-apical plane using a precision-cutting machine (Micracut 150 precision cutter; Metkon) followed by grinding and polishing using 800-grit silicon carbide paper. The central section of each block was stained (Stevenel blue and van Gieson picrofuchsin) and histologically evaluated with a light stereomicroscope (BX61; Olympus Corp) equipped with a high-resolution digital camera (E330; Olympus Corp).

The amount of new bone formation was identified as the distance filled by mineralized bone infiltration, starting from the surface of the defect wall and extending into the porosity of the scaffold (Fig. 3A). Scaffolds had higher amount of macroscopic porosities, which enabled the detection of bone-scaffold interface. All areas of new bone formation were isolated from each section to allow precise measurement of new bone formation (Fig. 3B). One experienced histomorphometric examiner (M.N.A.) examined the sections and measured new bone formation in a single session. The examiner repeated the measurements of the same sections in a different order, blindly, and interexaminer reliability was evaluated. The Student *t* test was used for data analysis (n=14, $\alpha$=.05) using computer software (SPSS Statistics, v14.0; SPSS Inc).

## RESULTS

Interexaminer reliability was 0.92, which indicated accurate evaluation and interpretation of new bone formation measurements. The Levene test for equality of variances (F=0.03, *P*<.86) indicated equality of variances between the tested groups. Degree of freedom in this study was 26. Examination of the scaffolds before addition of HA particles revealed average porosity of 77% and 2 average pore sizes, 59 μm and 540 μm. This porosity dropped to 43% after addition of HA particles, and the resultant pore sizes dropped to 28 μm and 211 μm. Calcium and phosphate peaks were identified inside the examined porosities. The density of the controls was 0.35 g/cm$^3$ and 0.68 g/cm$^3$ for the enriched scaffold (Table 1).

Histomorphometric analysis revealed that the scaffolds enriched with calcium phosphate had significantly (t=4.4, *P*<.001) higher new bone formation penetrating into the scaffolds (1.3 ±0.33 mm) than the controls (0.7 ±0.39 mm). The direction of bone formation was observed to infiltrate from the periphery surfaces of the scaffolds toward its center, and it started by first lining the pores and then gradually occupying its entire volume (Fig. 4). Clear marks of demarcation separating the edges of the inserted scaffolds from the jaw defects were detected, which became less marked after complete healing (Fig. 3). Entrapped HA spots were observed inside the pores of the enriched scaffolds. These HA islands were surrounded by partially mineralized bone. After 8 weeks, approximately one-third of the outer surface of the scaffolds was observed to degrade.

## DISCUSSION

A scaffold should have certain requirements that ideally help to serve the host site. It should allow infiltration of progenitor/stem cell for cellular proliferation and successful in-growth,[28,29] which depends mainly on the physical and chemical properties of the scaffold and on

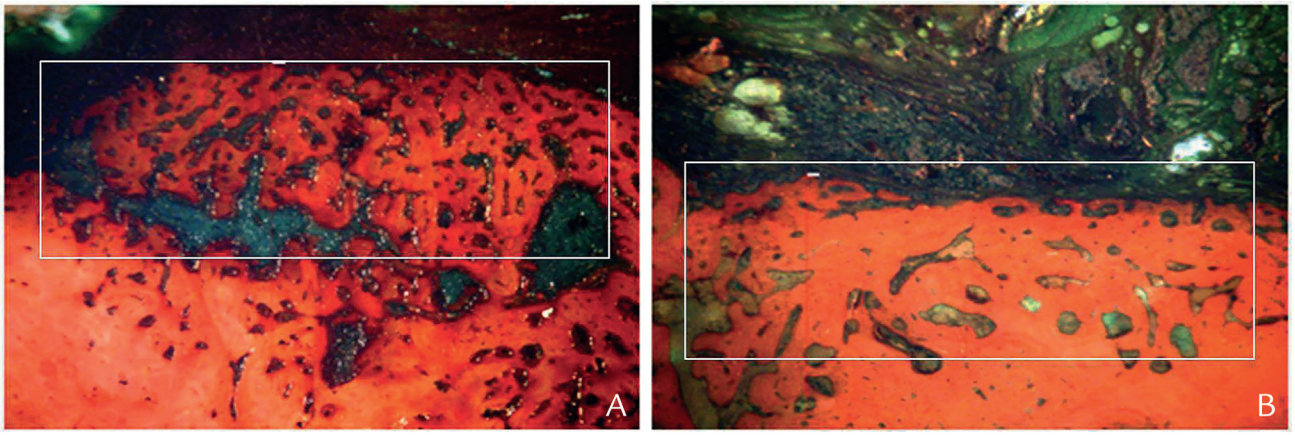


**Figure 4.** A, Histological section demonstrating new bone growth in HA-enriched PLA scaffold. White window marks area of new bone formation. B, Histological section demonstrating new bone growth in control PLA scaffold. White window marks area of new bone formation and height of new bone formation measured from surface of defect wall.

the percentage of the porosity and pore size and distribution. However, an ideal scaffold should fulfill other properties including biocompatibility, osteoconductivity, and osteoinductivity and should enhance cell attachment, suitable degradation rate, and mechanical properties close to those of natural bone. No scaffold has been proven to fulfill all these properties.[29,30]

Digital technology has improved the design and fabrication of different bioactive materials. Accurate image acquisition techniques such as cone beam computer tomography allow construction of 3D models of the defect size which could be easily transferred to CAD-CAM systems, allowing design and milling of the required scaffold. Accurate fit guarantees proper accommodation of the scaffold in the defect and proper sealing of the margins which will spare the surgeon time and effort required to customize either the scaffold or the defect size.

Both PLA and HA have been widely used in various biomedical applications. Owing to the weak mechanical properties and inflammatory and allergic reactions of PLA, HA has been added to improve the properties of PLA scaffolds.[31] Poly(lactic-co-glycolic acid) (PLGA)/nano-fluorohydroxyapatite composite scaffold showed that PLGA/nano-fluorohydroxyapatite composite scaffold with a ratio of 4:1 exhibited the best mechanical properties and proper porosity for bone regeneration. Also, it was found that cell viability was increased compared with PLGA.[32] A similar mixing ratio was used in this study.

A previous study[33] was concerned with evaluating the effectiveness of inserting a 3D bioresorbable polycaprolactone scaffold in fresh extraction sockets for improving bone healing and ridge preservation. The scaffolds were manually shaped by a surgeon using a scalpel. Porous scaffolds (70% porosity) were associated with more favorable bone growth which is in accordance with the present results in which a higher porosity ratio was achieved using 2 levels of pore sizes, micro and macro pores resulting in enhanced osteogenesis capacity. The null hypothesis was thus rejected.

Degradation of the PLA starts with an autocatalytic random hydrolysis reaction leading to the scission of the ester linkages. The second mechanism is due to loss of weight and mechanical strength as a result bioerosion that increases the exposed surface area. During this process, calcium salts are released in the surrounding media and start to enhance the process of osteogenesis. The rate of degradation (5 to 6 months) should be close to that of bone formation to optimize the performance of the scaffolds.[33] However, absence of calcium salts during degradation of the scaffold resulted in poor bone growth and infiltration rate falling behind the faster rate of soft tissue growth which explains the poor behavior of the controls. Further studies are needed to optimize biodegradation rate of the scaffolds and to improve mineralization of deposited bony matrix to enhance clinical performance and reduce healing time.

## CONCLUSIONS

Within the limitation of this in vivo study, the following conclusion was drawn:

1. HA and β-TCP enhanced osteogenesis of porous PLA scaffold.

## REFERENCES

1. Lekovic V, Camargo PM, Klokkevold PR, Weinlaender M, Kenney EB, Dimitrijevic B, et al. Preservation of alveolar bone in extraction sockets using bioabsorbable membranes. J Periodontol 1998;69:1044-9.
2. Gultekin BA, Bedeloglu E, Kose TE, Mijiritsky E. Comparison of bone resorption rates after intraoral block bone and guided bone regeneration augmentation for the reconstruction of horizontally deficient maxillary alveolar ridges. Biomed Res Int 2016:4987437.

3. Roccuzzo M, Ramieri G, Bunino M, Berrone S. Autogenous bone graft alone or associated with titanium mesh for vertical alveolar ridge augmentation: a controlled clinical trial. Clin Oral Implants Res 2007;18:286-94.
4. Benic GI, Joo M-J, Yoon S-R, Cha J-K, Jung U-W. Primary ridge augmentation with collagenated xenogenic block bone substitute in combination with collagen membrane and rhBMP-2: a pilot histological investigation. Clin Oral Implants Res 2017;28:1543-52.
5. Nazirkar G, Singh S, Dole V, Nikam A. Effortless effort in bone regeneration: a review. J Int Oral Health 2014;6:120-4.
6. Jun SH, Ahn JS, Lee JI, Ahn KJ, Yun PY, Kim YK. A prospective study on the effectiveness of newly developed autogenous tooth bone graft material for sinus bone graft procedure. J Adv Prosthodont 2014;6:528-38.
7. Hosseinpour S, Ahsaie MG, Rad MR, Taghi Baghani M, Motamedian SR, Khojasteh A. Application of selected scaffolds for bone tissue engineering: a systematic review. J Oral Maxillofac Surg 2017;21:109-29.
8. Kumar P, Vinitha B, Fathima G. Bone grafts in dentistry. J Pharm Bioall Sci 2013;5:125-9.
9. Dong L, Wang SJ, Zhao XR, Zhu YF, Yu JK. 3D- Printed poly(ε-caprolactone) scaffold integrated with cell-laden Chitosan hydrogels for bone tissue engineering. Sci Rep 2017;7. 13838-7.
10. Vats A, Tolley NS, Polak JM, Gough JE. Scaffolds and biomaterials for tissue engineering: a review of clinical applications. Clin Otolaryngol 2003;28: 165-72.
11. LeGeros RZ. Calcium phosphate-based osteoinductive materials. Chem Rev 2008;108:4742-53.
12. Salgado AJ, Coutinho OP, Reis RL. Bone tissue engineering: state of the art and future trends. Macromol Biosci 2004;4:743-65.
13. García-Gareta E, Coathup MJ, Blunn GW. Osteoinduction of bone grafting materials for bone repair and regeneration. Bone 2015;81:112-21.
14. Wopenka B, Pasteris JD. A mineralogical perspective on the apatite in bone. Mater Sci Eng C 2005;25:131-43.
15. Hu Y, Grainger DW, Winn SR, Hollinger JO. Fabrication of poly (α-hydroxy acid) foam scaffolds using multiple solvent systems. J Biomed Mater Res 2002;59:563-72.
16. Schieker M, Seitz H, Drosse I, Seitz S, Mutschler W. Biomaterials as scaffold for bone tissue engineering. Eur J Trauma Emerg Surg 2006;32:114-24.
17. Hamad K, Kaseem M, Yang HW, Deri F, Ko YG. Properties and medical applications of polylactic acid: a review. Express Polym Lett 2015;9: 435-55.
18. Gentile P, Chiono V, Carmagnola I, Hatton PV. An overview of poly (lactic-co-glycolic) acid (PLGA)-based biomaterials for bone tissue engineering. Int J Mol Sci 2014;15:3640-59.
19. Santoro M, Shah SR, Walker JL, Mikos AG. Poly (lactic acid) nanofibrous scaffolds for tissue engineering. Adv Drug Deliv Rev 2016;107:206-12.
20. Murakami N, Saito N, Horiuchi H, Okada T, Nozaki K, Takaoka K. Repair of segmental defects in rabbit humeri with titanium fiber mesh cylinders containing recombinant human bone morphogenetic protein-2 (rhBMP-2) and a synthetic polymer. J Biomed Mater Res 2002;62:169-74.
21. Chang PC, Liu BY, Liu CM, Chou HH, Ho MH, Liu HC, et al. Bone tissue engineering with novel rhBMP 2-PLLA composite scaffolds. J Biomed Mater Res A 2007;81:771-80.
22. Bhumiratana S, Bernhard JC, Alfi DM, Yeager K, Eton RE, Bova J, et al. Tissue-engineered autologous grafts for facial bone reconstruction. Sci Transl Med 2016;8:34-6.
23. Buser D, Dula K, Hirt HP, Schenk RK. Lateral ridge augmentation using autografts and barrier membranes: a clinical study with 40 partially edentulous patients. J Oral Maxillofac Surg 1996;54:420-32.
24. Mangano F, Zecca P, Pozzi-Taubert S, Macchi A, Ricci M, Luongo G, et al. Maxillary sinus augmentation using computer-aided design/computer-aided manufacturing (CAD/CAM) technology. Int J Med Robot 2013;9:331-8.
25. Liu YF, Xu LW, Zhu HY, Liu SS. Technical procedures for template-guided surgery for mandibular reconstruction based on digital design and manufacturing. Biomed Eng Online 2014;13:63.
26. Figliuzzi M, Mangano FG, Fortunato L, De Fazio R, Macchi A, Iezzi G, et al. Vertical ridge augmentation of the atrophic posterior mandible with custom-made, computer-aided design/computer-aided manufacturing porous hydroxyapatite scaffolds. J Craniofac Surg 2013;24:856-9.
27. Aboushelib MN, Shawky R. Osteogenesis ability of CAD/CAM porous zirconia scaffolds enriched with nano-hydroxyapatite particles. Int J Implant Dent 2017;3:21.
28. Bertoldi S, Farè S, Tanzi MC. Assessment of scaffold porosity: the new route of micro-CT. J Appl Biomater Biomech 2011;9:165-75.
29. Lee DH, Tripathy N, Shin JH, Song JE, Cha JG, Min KD, et al. Enhanced osteogenesis of β-tricalcium phosphate reinforced silk fibroin scaffold for bone tissuebiofabrication. Int J Biol Macromol 2017;95:14-23.
30. Zhang L, Morsi Y, Wang Y, Li Y, Ramakrishna S. Review scaffold design and stem cells for tooth regeneration. Jap Dent Sci Rev 2013;49:14-26.
31. Zhang H, Mao X, Du Z, Jiang W, Han X, Zhao D, et al. Three dimensional printed macroporous polylactic acid/hydroxyapatite composite scaffolds for promoting bone formation in a critical-size rat calvarial defect model. Sci Technol Adv Mater 2016;17:136-48.
32. Antikainen T, Ruuskanen M, Taurio R, Kallioinen M, Serlo W, Törmälä P, et al. Polylactide and polyglycolic acid-reinforced coralline hydroxy-apatite for the reconstruction of cranial bone defects in the rabbit. Acta Neurochir 1992;117:59-62.
33. Go BT, Teoh LY, Tan DB, Zang Z, Teo SH. Novel 3D polycaprolactone scaffold for ridge preservation-a pilot randomized controlled clinical trial. Clin Oral Implants Res 2015;26:271-7.



**Corresponding author:**
Dr Moustafa Aboushelib
Biomaterials Department
Faculty of Dentistry
Alexandria University
Champollion St
Azarita, Alexandria
EGYPT
Email: moustafaaboushelib@gmail.com



https://doi.org/10.1016/j.prosdent.2018.03.033